

Chimia 52 (1998) 3–9
 © Neue Schweizerische Chemische Gesellschaft
 ISSN 0009–4293

Lessons from Nature

Koji Nakanishi* and Nina Berova

Abstract. Terrestrial and marine animals, plants, insects, and microorganisms produce a large variety of compounds for the organism's development, daily survival, self-defence, symbiosis, sexual attraction, *etc.* Certain of these compounds are discussed here, with emphasis not only on their isolation and structure determination, but also on the question as to why they are active. This requires a multidisciplinary approach, for a better understanding of life's processes and nature's mysteries.

1. Introduction

The chemistry dealing with natural products, not to mention ancient times, but in the modern era as well, is the oldest branch in organic chemistry. It started with a curiosity regarding biological activity, folk medicinal cures, odor, *etc.*, which in the early days of modern chemistry was focused on isolation and subsequent structure determinations. This was followed by synthesis and elucidation of biosynthetic routes. With the rapid advancement in chromatographic isolation techniques and spectroscopy, determination of structures became quite routine in most cases. Following the early period of random isolation, the trend shifted towards more logical activity-monitored isolation.

However, in recent years, it has become possible for organic chemists to direct their attention towards the origin of bioactivity, which almost invariably involves the interaction between ligand and its biopolymeric receptor; a decade ago, such studies were impossible to be performed on a molecular structural level. Organic chemists, especially those involved in structural studies, have the techniques and knowledge as to how to approach such studies, but on the other hand lack the knowledge where exciting problems exist. In contrast, biologists and medical doctors are daily exposed to exciting phenomena, but often do not think that the phenomena could be clarified on a chemical basis. Nature is extremely clever but complex, and it is only with multidisciplinary collaborative research that such natural phenomena can be investigated. A question such as why does sugar give the sensation of sweetness is far from being understood on a ligand/receptor basis. We are just at the starting point of an interdisciplinary approach to clarify such problems. Examples dealing with straight isolation/structural studies to more recent mode of action studies are given in the following.

2. Ginkgolides

The ginkgo (*Ginkgo biloba* L.) is the last surviving member of a family of trees which appeared more than 250 million years ago (Paleozoic) and reached their climax during the Jurassic period. During the last few million years, all species excepting *Ginkgo biloba*, which is believed to have remained unchanged for the last 150 million years, have become extinct.

These are diterpenes with an aesthetic cage skeleton with six five-membered rings, *i.e.*, a spiro[4.4]nonane carbocyclic ring, three lactones, and a tetrahydrofuran ring [1][2]. It is probably still the only terpenoid to carry a *tert*-butyl group (*Fig. 1*). Although the NMR (all spectra measured in the mild solvent TFA) always showed a nine-proton singlet at 1.2–1.3 ppm, pres-

*Correspondence: Prof. K. Nakanishi
 Department of Chemistry
 Columbia University
 New York, NY 10027, USA
 Tel.: +1 212 854 2169
 Fax: +1 212 932 8273

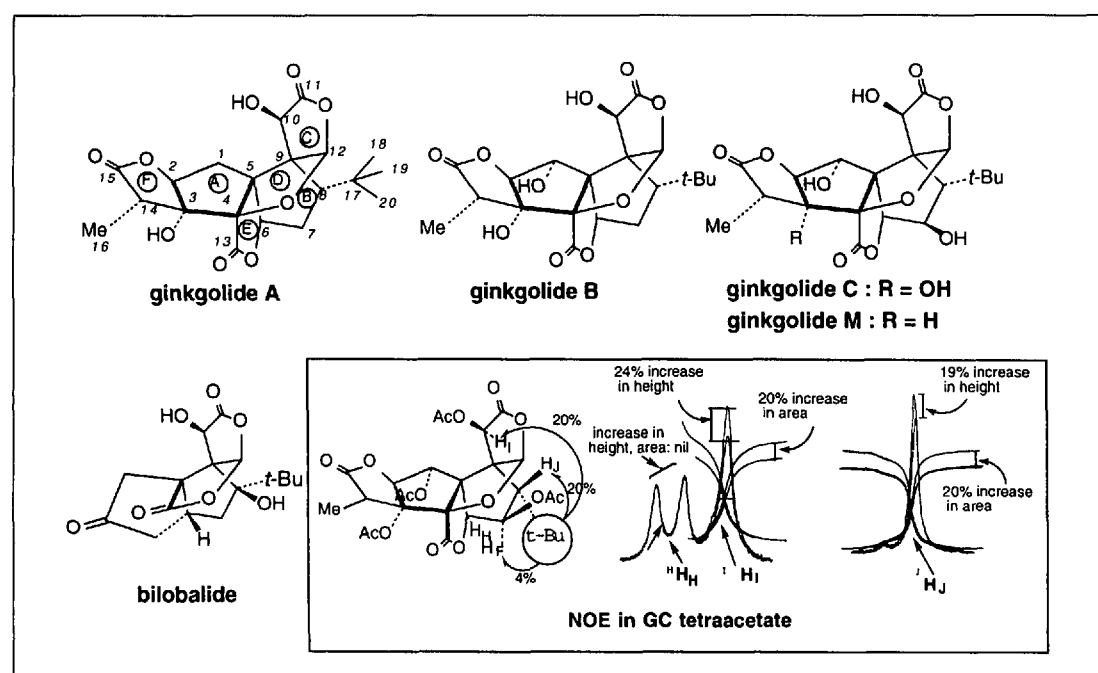


Fig. 1. The ginkgolides and NOEs

ence of the *t*-Bu group was established only after detection of a *t*-Bu peak in the HRMS at 57.074 and isolation of pivalic acid, characterized as a crystalline derivative upon *Kuhn-Roth* oxidation. The sesquiterpenoid bilobalide structure was determined later in collaboration with the groups of *Major* (Virginia) and *Bähr* (Heidelberg) [3].

Although no special biological activity was found for these molecules at the time of structural studies, potent inhibitory activity against platelet-activating factor was found subsequently, especially for ginkgolide B. It is remarkable that *Ginkgo biloba* is already mentioned in the Chinese materia medica in 2800 B.C., and that today the sales of the crude extract, reput-

ed to improve memory and sharpen mental focus, is 2–3 billion dollars as a dietary supplement throughout the world.

Structural studies were performed in the traditional classical fashion in which many (*ca.* 50) derivatives were prepared and submitted to 100 MHz NMR, IR, CD, and other measurements. The root-bark extract collected from typhoon-damaged trees (100 kg) gave after chromatography and a tedious 10–15-step fractional recrystallization 10 g each of ginkgolide A (GA) and B (GB), 20 g of GC, and 200 mg of GM. Purification of ginkgolides were seriously hampered by their remarkable tendencies to exhibit polymorphism and form mixed crystals; recently, *van Beek* and *Lelyveld* have devised an efficient

preparative scale isolation scheme using medium-pressure liquid chromatography [4].

The NMR of the ginkgolides are too simple because the connectivity of proton groups are blocked by the presence of quaternary carbons. Without much thought GA was reduced with LAH (= LiAlH₄) which not surprisingly yielded a 'useless' syrup; however, drying of the syrup, which accidentally contained a trace of acid, gave rise to a solid, *i.e.*, 'GA triether' (the ring D ether makes it a tetraether), which became *the* critical compound for structural studies. Namely, the LAH reduction introduced additional protons which necessarily made the NMR more complex leading to more connectivities. Exhaustive decoupling studies of the NMR of GA triether and other derivatives, especially *t*-Bu decoupling, led to what is now understood as NOE. Although NOE was still unknown at that time, it was correctly assumed to be due to signal enhancement arising from irradiation of a nearby proton and played a key role in structural deductions [1e] (*Fig. 1*); *Anet* and *Bourn*'s first paper on NOE appeared during these structural studies [5]. A comparison of the complex triether and simple GA spectra showed that except for the newly introduced six protons, the spectra are quite similar; the similarity was confirmed by the 'GA triether-d₆' spectrum resulting from LAD (= LiAlD₄) reduction in which all six newly introduced peaks disappeared (see middle NMR trace in *Fig. 2*). This indicated that despite the difference between three lactones and three ether rings, remarkably, the original ring structure was retained in the triether; this also was the first indication that three lactones were present.

The fact that LAH reduction of GA followed by pyrolysis of the octaol results in recyclization to the original cage skeleton demonstrated the unique stability of the beautiful cage structure. The following transformations also show the remarkable stability of the ginkgolide structure. Thus, alkali fusion of 300 mg GA merely results in expulsion of two carbons, captured as oxalic acid, and generation of the hemiacetal, bisnor-GA (*Scheme*).

A further unique set of reactions is the following. Treatment of an ice-cooled solution of 2 g of GA in concentrated sulfuric acid with sodium dichromate in 50% sulfuric acid gave a green solution which upon pouring into ice-water gave 1.7 g of crystals of dehydro-GA, which were recrystallized from dilute acetone (fine needles, 670 mg, sublimed at 180°/10 mmHg). However, dehydro-GA, the oxolactone, was a source of confusion which led us to

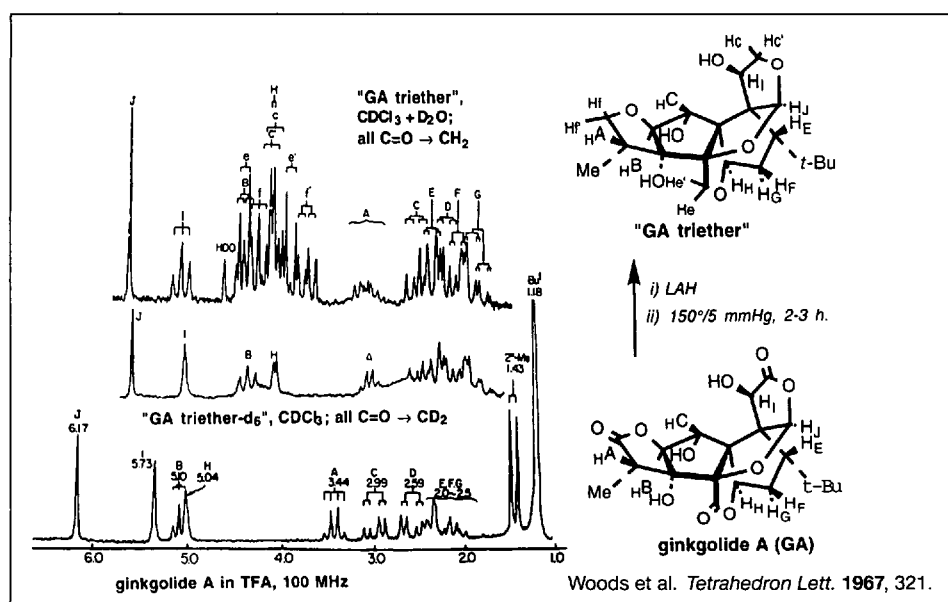
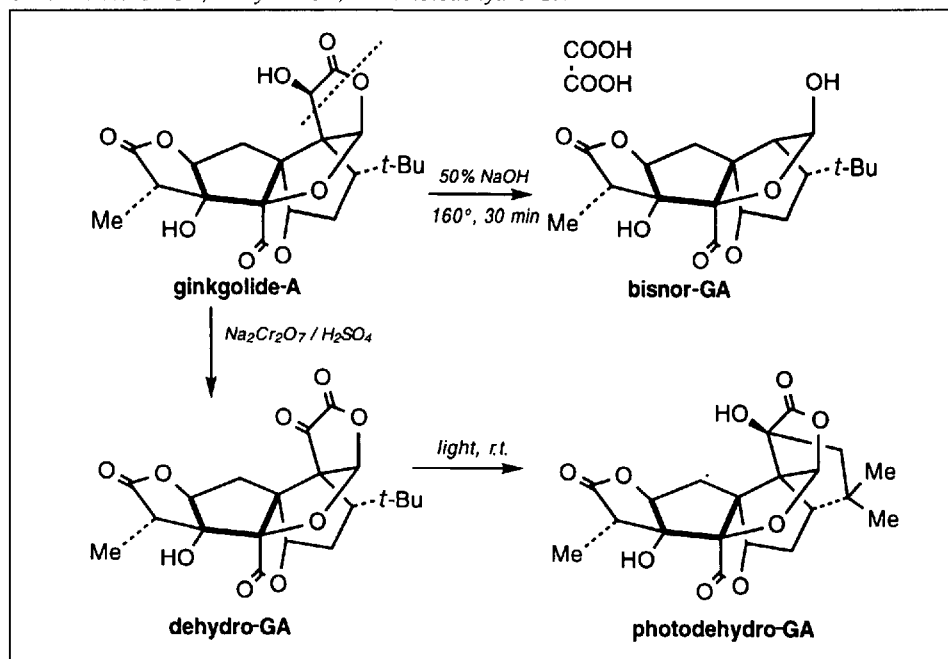


Fig. 2. NMR of ginkgolide A, GA triether, and GA triether-d₆

Scheme. *Bisnor-GA*, *Dehydro-GA*, and *Photodehydro-GA*



consider a wrong structure for a while. Namely, since we had suspected the presence of a hydroxy lactone, the oxidation was to yield an oxolactone. The NMR of dehydro-GA was measured immediately and therefore showed the familiar nine-proton singlet which was present in all ginkgolide spectra. However, if this were an α -keto lactone it should demonstrate weak but distinct UV bands typical for 1,2-dicarbonyls, and be accompanied by ORD Cotton effects around 400 nm, which was not the case. It was thus concluded that the oxidation product must be a tetra-lactone. What happened was that ORD and UV, because of the psychological barrier in measuring them (the samples had to be weighed!) relative to NMR, were measured with a sample that had been left for some time, during which period the photocyclization to photodehydro-GA had taken place; the photocyclization occurs even during TLC. Only when the NMR of a dehydro-GA sample left around was remeasured in a different solvent to gain further information, did it become clear that the *t*-Bu group had disappeared and had been replaced by two Me groups. The unusual spectroscopic and photochemical properties of dehydro-GA were subsequently clarified.

Ginkgo biloba callus was successfully grown by adding 2,4-dichlorophenoxyacetic acid to an agar culture of its embryo containing appropriate nutrients. Preliminary biosynthetic studies with labeled precursors also demonstrated the gross biosynthetic pathway [6]. However, more recent biosynthetic studies performed in Arigoni's group in Zurich has shown that these ancient ginkgolides are one of the first members of a newly emerging class of terpenoids which do not follow the mevanolate pathway [7].

3. The CD Exciton Chirality Method

The determination of molecular chirality is becoming increasingly important due to the importance of acquiring a better insight of the stereochemical aspects factors involved in bioactivity. The CD exciton chirality method has proven to be a very sensitive, simple, and versatile microscale tool for elucidating absolute configuration and detecting subtle conformational changes in a wide variety of natural and synthetic compounds containing two or more chromophores [8]. However, its potential in structural studies has yet to be explored.

The through-space interaction of the electric transition moments of two identi-

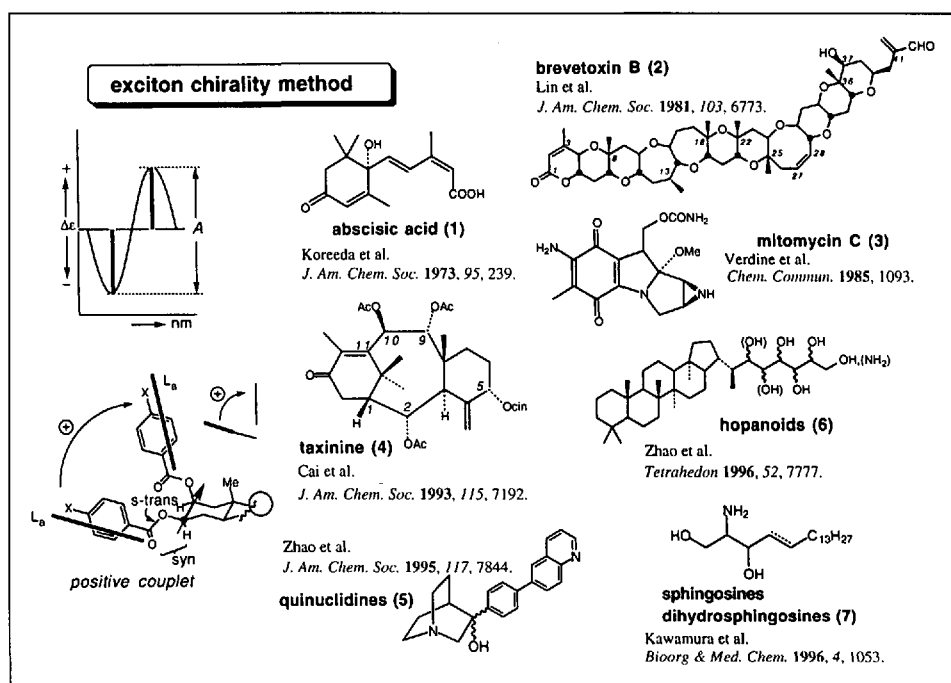


Fig. 3. Exciton chirality: examples

cal chromophores gives rise to an exciton-coupled 'split' CD spectrum or 'bisignate curve'. For example, in the case of the bis-*p*-substituted benzoate shown in Fig. 3, the absolute sense of twist of the two transition moments, which constitute a clockwise chirality, give rise to the depicted bisignate CD which is defined as positive. The time-averaged acylate conformation (CD is a time-averaged spectrum) is fixed in an *s-trans* ester bond with the carbonyl and carbinyl proton in *syn*-conformation. The amplitude (*A* value) of the split CD curve is: *i*) inversely proportional to the square of the interchromophoric distance; *ii*) proportional to the chromophoric absorption-extinction coefficient; and *iii*) dependent on the interchromophoric projection angle with a maximum at *ca.* 70° and minima at 0° or 180° (for 1,2-acylates). These trends still hold for molecules containing different chromophores, except that the exciton-coupled CD curves cover the range encompassing the different absorption maxima. Moreover, coupling is still observed even when the absorption maxima of chromophores are 100 nm apart. The sign of the exciton-coupled split CD, reflecting the spatial arrangement of the chromophores, leads to the assignment of the absolute configuration (or conformation) in a non-empirical manner, *i.e.*, a positive bisignate CD is associated with a positive absolute twist between the interacting electric transition moments, and *vice versa*. In rigid systems, the assignment of absolute configurations is straightforward. However, in acyclic systems, such as acyclic poly-

ols, the assignment of absolute configuration is more challenging due to possible equilibrium between several different conformers.

Fig. 3 shows some examples leading to determination of absolute configurations.

Abscisic Acid (1). The CD of the underivatized compound itself shows coupling between the enone and dienoic-acid moieties, which leads to the assignment of absolute configuration.

Brevetoxin (2). The 27-ene compound was converted into a *cis*-1,2-glycol, and its relative configuration was determined by NMR together with the conformation of the eight-membered ring. The CD of the dibenzoate determined the absolute configuration.

Mitomycin C (3). *Trans*-opening of the aziridine ring yielded the amino alcohol which was derivatized with the red-shifted chromophore *p*-methoxycinnamate to avoid overlap with the amino-quinone moiety.

Taxinine (4). Here again the C(9) and C(10) hydroxy functions were derivatized with red-shifted chromophores which did not overlap with the twisted enone chromophore.

Quinuclidines (5). The quinuclidine nitrogen of the bicyclic system was converted into a quaternary ammonium salt by attaching the *p*-phenylbenzyl moiety, the absorption band of which overlaps with the existing chromophore thus leading to exciton coupling. The pendant benzylic chromophore can adopt three equal conformers with respect to the quinuclidine nucleus, but the conformer with the

benzyl group in the south 'triant' dominates the sign of the CD couplet due to its favorable angle and distance with the existing quinolinylphenyl chromophore.

Hopanoids (6). Reference CD curves of a homologous series of 1,2-polyols up to pentols (the Fischer sugar family tree) derivatized as anthroates at C(1)-OH and *p*-methoxycinnamates at the remaining hydroxy groups showed a systematic trend that greatly simplified assignments of relative and absolute configurations; the same trend also holds for corresponding 1-amino-polyols [9]. Comparison with the library lead to hopanoid side-chain configurational assignments.

Sphingosines (7). A simple scheme was developed which involved conversion of the amino group into the fluorescent and stable naphthimido chromophore, followed by conversion of the primary and secondary hydroxy groups into fluores-

cent 2-naphthoate esters. The fluorescence of these chromophores allows the reactions to be performed at submicrogram levels leading to establishment of all eight absolute configurations of stereoisomers (the CD of dihydro series differ from those of the sphingosines).

The exciton chirality method has recently been applied to determine the absolute sense of twist of the retinal chromophore within the visual pigment rhodopsin (see below).

4. Exciton Chirality in Fluorescence-Detected CD (FDCD); Sensitivity Enhancement

Chromophores with intense absorptions allow CD detection of exciton-coupled CD at much lower concentrations since the amplitude is proportional to ϵ^2 .

Furthermore, fluorescent chromophores, e.g., 2-anthroate (UV λ_{max} 258 nm (ϵ 93,000), λ_{ex} 270 nm, λ_{em} 438 nm) greatly facilitate the handling and sample purification [10]. However, although fluorescence greatly enhances HPLC detection, the sensitivity of CD detection (obtained in transmission) remains limited because it depends on the intensity of dichroic absorption. In order to further enhance the CD sensitivity and to enable the CD detection of ng- μ g scale material, a prototype fluorescence detector was attached to a regular CD JASCO-720 model and the CD was measured through fluorescence detection, based on the formalism described by Tinoco *et al.* [11]. The fluorescence detection resulted in significant sensitivity enhancement.

For example, in the case of the bis(6-methoxy-2-naphthoate) derivative, which exhibits intense fluorescence at 361 nm with a quantum yield of 0.64, the corresponding enhancement is 100-fold [12]. As shown (Fig. 4, a), the experimental exciton split CD spectrum of **8** ($c = 4.37 \times 10^{-6}$ M; $\lambda_{\text{ext}}(\Delta\epsilon)$, 254.8 nm (+147.4)/234.4 nm (-124.3), $A_{\text{CD}} = +271.7$) can be simulated satisfactorily from the experimental FDCD curve (at the same concentration) giving rise to a CD with extrema at 255.4 nm (+129.4) and 233.8 nm (-120.2), $A_{\text{CD}} = +249.5$. However, when diluted 100-fold ($c = 4.37 \times 10^{-8}$ M), as presented in (b), the signal-to-noise ratio of normal CD becomes very low ($S/N = 2$), while the CD converted from FDCD still shows a clear exciton couplet, although of slightly lower intensity, with $\lambda_{\text{ext}}(\Delta\epsilon)$ 254.0 nm (+120.8)/233.2 nm (-98.3), $A_{\text{CD}} = +219.1$. The excellent agreement seen between the CD and FDCD spectra suggests that a similar exciton coupling mechanism is operating. Although FDCD still requires further studies for a better understanding of basic principles, these preliminary results are very promising. They demonstrate that FDCD measurements of exciton coupling between strongly absorbing and fluorescent chromophores can provide an extremely sensitive tool for structural studies at very low levels of sample, e.g., picogram levels under favorable conditions.

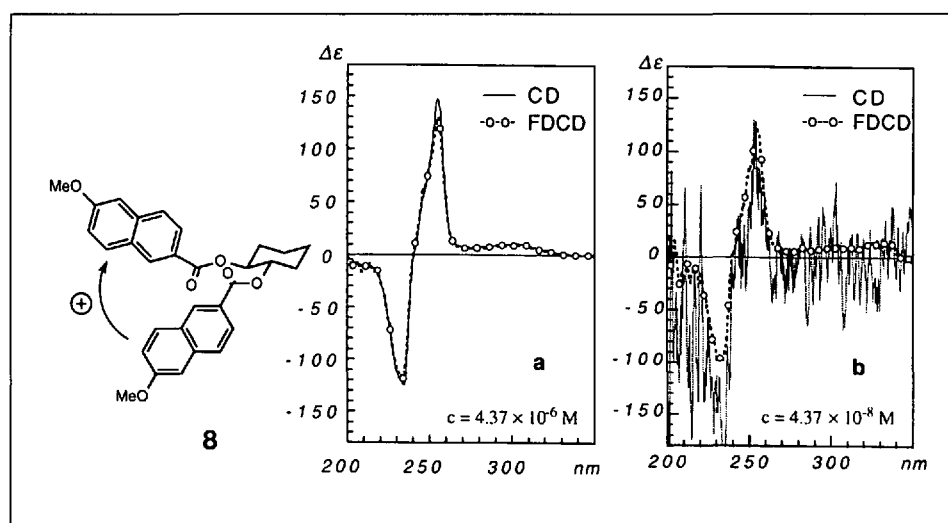


Fig. 4. a) CD of **8** (in MeCN), 4.37×10^{-6} M. Solid line shows conventional CD; line with circles shows CD derived from FDCD. b) CD of **8** (in MeCN), $c = 4.37 \times 10^{-8}$ M. Noisy line shows conventional CD, $S/N = 2$; the CD derived from FDCD (Fig. 4, b), line with circles, still exhibits clear exciton coupling.

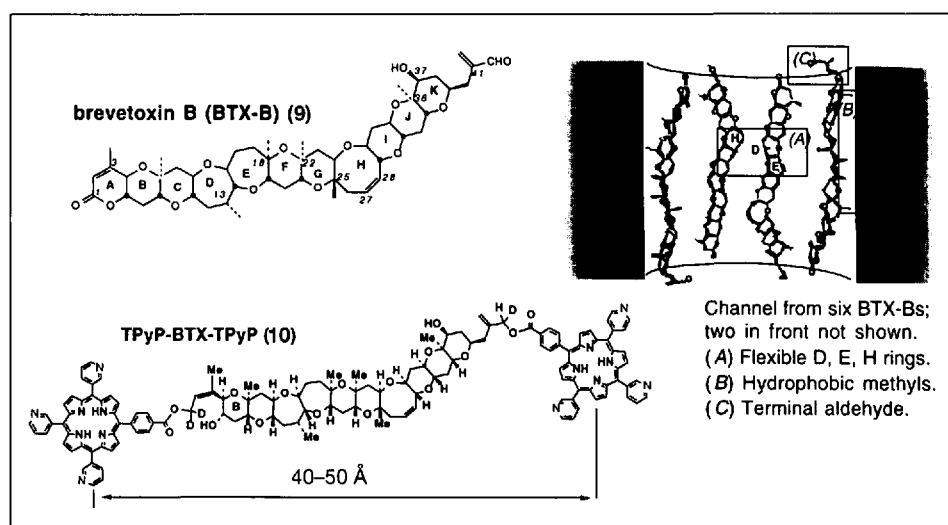


Fig. 5. Brevetoxin (**9**), hydrophilic TPyP-BTX-TPyP (**10**), BTX channel

5. Self-Assembled Brevetoxin-Porphyrin Conjugates

Brevetoxins, involved in the 'red tide' as well as shellfish poisoning, are known to bind to cell membranes and membrane proteins. Brevetoxin B (BTX-B, **9**) [13] interacts specifically with neuronal sodi-

um channels. However, it was found that BTX also induces selective ion movements across lipid bilayers through transmembrane BTX self-assemblies [14a].

The supramolecular chemistry involved in the interaction of BTX with itself, cations, and lipid bilayers was studied using the powerful porphyrin chromophores as CD labels such as the hydrophilic tripyridyl-porphyrinyl TPyP-BTX-B-TPyP (**10**) and other hydrophobic and fluorescent derivatives [14b]. The structure of the active BTX-B complex in lipid bilayers is a cyclic, transmembrane self-assembly consisting of antiparallel aligned BTX molecules; similar ionophoric BTX self-assemblies have also been characterized in MeOH/water. In Fig. 5, it is arbitrarily assumed that *ca.* six molecules form a cylinder (two in the front are not depicted). Structural studies have shown that the critical 'micelle' concentrations (*cmc*) of different BTXs dictate specific mechanisms of pore formation. Although the distance between the two porphyrins in TPyP-BTX-B-TPyP (**10**) is 40–50 Å, the two porphyrin moieties still interact through space in water, pH 4, and give rise to an exciton-coupled CD! [14b].

6. Philanthotoxin-433 and the Nicotinic Acetylcholine Receptor

The venom of *Philanthus triangulum F.*, a digger wasp found in the Sahara desert that preys on honeybees, blocks the quisqualate-sensitive glutamate receptor (qGlu-R) located post-junctionally on locust muscle and the nicotinic-acetylcholine receptor (nACh-R). The most active component of the venom, philanthotoxin-433 (δ -PhTX, numerals denote number of methylenes in the polyamine chain), was isolated from the venom glands of the female wasp and assigned the structure shown in Fig. 6, with a butyryl-tyrosyl-thermospermine sequence [15]. PhTX-433 is an efficient, noncompetitive, reversible antagonist of qGlu-R of invertebrate skeletal muscle and some vertebrate Glu-R that is thought to act by open channel block. *Ca.* 80 polyamine toxins have also been isolated from spider venoms and found to be potent antagonists of Glu-R and nACh-R [16]; two of the very early spider toxins to be characterized are shown in Fig. 6.

Over 100 synthetic analogs [17] coupled with photoaffinity studies with nACh-R using the radioactive bis-iodo(^{125}I) *p*-azidobenzamide analog has led us to propose a working tertiary model showing the ligand-receptor interaction (Fig. 7). Name-

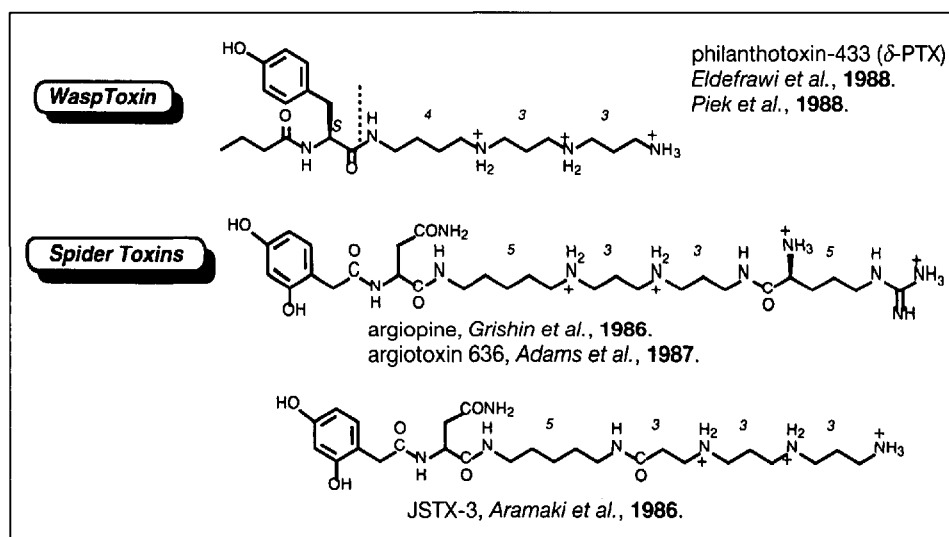


Fig. 6. Wasp-toxin philanthotoxin-433 (PhTX-433) and spider toxins

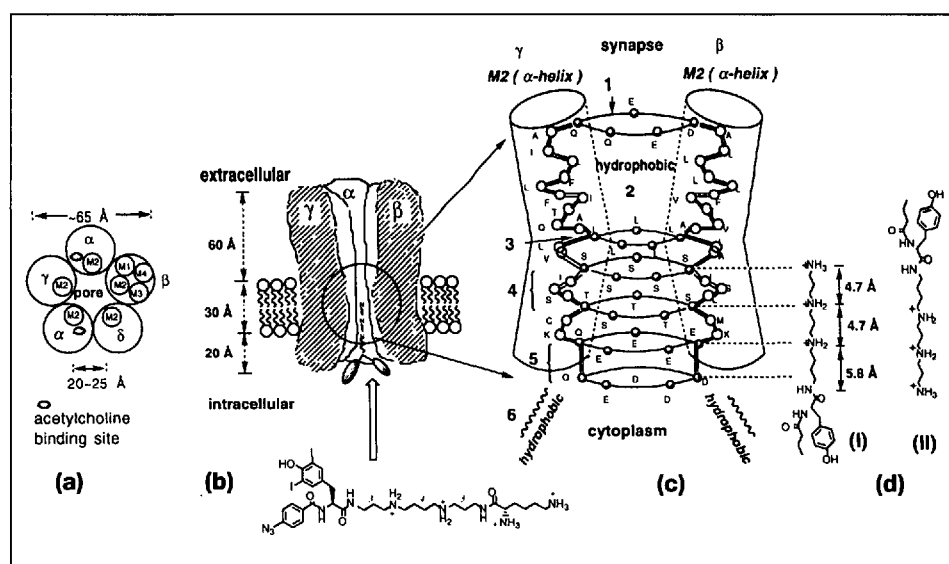


Fig. 7. a) Acetylcholine binding site (top view); b) cross section of nAChR showing the mode of binding of photoaffinity-labeled PhTX analog under the experimental conditions employed; c) enlarged transmembrane cross section showing the various domains; d) two orientations for matching PhTX against the hydrophilic rings of the transmembrane domains

ly, it is possible to line the polyamine 'tail' chain of PhTX against the hydrophilic rings in regions '4' and '5' of the receptor consisting of Ser, Thr, and anionic residues, while the Tyr, and butyryl moieties of PhTX ('head' group) are in the cytoplasmic hydrophobic region. The distances between the amino groups in PhTX is close to the 5.4 Å pitch of α -helices as connected schematically by the dotted lines (see (I) in Fig. 7). However, the photoaffinity-labeling studies were performed under conditions in which the synaptic and cytoplasmic sides of the nACh receptor were both accessible to the ligand. A separate study with analogs containing large hydrophobic aromatic groups or porphyrins instead of the Tyr and butyryl groups suggested that the mode of binding is with the head groups in the hydrophobic

cavity of the receptor (see (II) in Fig. 7 with the PhTX molecule flipped over). Top view of cross section of nACh-R showing the five transmembrane subunits (α , α , β , γ , δ); acetylcholine ligand binding sites are on the α subunit. Putative binding of the photolabile radioactive (^{125}I)philanthotoxin analog is indicated by the white arrow. Side view of the magnified transmembrane segment shows hydrophilic anionic ring 1, hydrophobic pocket 2, hydrophilic rings 3 and 4, anionic ring 5, and hydrophobic cytoplasmic region 6. The two possible modes of binding of the PhTX molecule are shown by arrangement (I) and (II).

Numerous subtypes of Glu-Rs are involved in learning, memory, Alzheimer's disease, and other neurological disorders. Because of the gross similarity between

the nACh-R and Glu-R structures, the knowledge gained from nACh-R should contribute in our understanding of the binding of the polyamine ligands to mammalian Glu-R, and suggest useful site-specific structural modifications in the synthetic ligands with potentialities as important drugs. Scaling down and streamlining of general techniques involved for investigating the mode of binding of PhTX analogs and other ligands to nACh-R, and if possible overexpressed Glu-Rs, are being developed.

7. The Mode of Binding of the Retinal Chromophore in Rhodopsin

Studies of retinal proteins containing retinal analogs have become an indispensable tool for the investigation of vision, phototaxis, ion transport, *etc.* Numerous retinal analogs have been made, incorporated into various retinal proteins, and submitted to a variety of biophysical, biochemical, and other studies [18].

We were engaged for many years to determine the location of the retinal chromophore in rhodopsin (bovine) in the static state. However, this led to unusual difficulties because besides rhodopsin being one of the most tedious of the membrane proteins to handle due its stickiness, photoaffinity labeling had to circumvent the photolability of the chromophore itself. This was finally solved by employing the tritiated photoaffinity analog in which the 11-*cis*-to-*trans* isomerization is blocked via a six-membered ring bridging C(10) and C(13) (*Fig. 8*, the bridge prevents complications due to isomerization during photolysis of the photoaffinity label). The carbene generated at C(3) cleanly cross-linked to two amino-acid residues, Trp-265 and Leu-266, *i.e.*, the ionone C(3)/C(4) is close to helix F of the seven transmembrane α -helices in the unexcited dark state [19]. This finding is of prime importance in elucidating the subsequent structural changes occurring in the visual pigment leading to vision. *Nakayama* and *Khorana* performed photoaffinity labeling using a retinal analog with a trifluoromethyl-diazerene group in which the 11,12-ene was not locked; this resulted in cross-linking to the same Trp-265 and Leu-266, together with several other amino acids in helix C [20]; since isomerization to the all-*trans*-chromophore is not blocked in this case, the affinity-labeling results would suggest that light-induced isomerization moves C(3) and C(4) of the ionone ring to come in contact with helix C by movements of the chromophore and the receptor, especially helices C and F. This movement, which is central to our understanding of the transduction process on a rigid molecular structural basis is under study. In connection with this, diazoketo retinal analog without the bridging six-membered ring in the side chain has been successfully prepared by submitting the all-*trans*-diazoketo to retinochrome, the isomerase present in squid eyes which transforms all-*trans*-retinal into 11-*cis*; isomerization occurred in 50% yield [21]. This photoaffinity label will now be incorporated into rhodopsin, and photoaffinity studies will be performed in liquid nitrogen to examine the cross-linking at the bathorhodopsin stage, *i.e.*, the first sequestable intermediate in the transduction process.

The carbene generated at C(3) cleanly cross-linked to two amino-acid residues, Trp-265 and Leu-266, *i.e.*, the ionone C(3)/C(4) is close to helix F of the seven transmembrane α -helices in the unexcited dark state [19]. This finding is of prime importance in elucidating the subsequent structural changes occurring in the visual pigment leading to vision. *Nakayama* and *Khorana* performed photoaffinity labeling using a retinal analog with a trifluoromethyl-diazerene group in which the 11,12-ene was not locked; this resulted in cross-linking to the same Trp-265 and Leu-266, together with several other amino acids in helix C [20]; since isomerization to the all-*trans*-chromophore is not blocked in this case, the affinity-labeling results would suggest that light-induced isomerization moves C(3) and C(4) of the ionone ring to come in contact with helix C by movements of the chromophore and the receptor, especially helices C and F. This movement, which is central to our understanding of the transduction process on a rigid molecular structural basis is under study. In connection with this, diazoketo retinal analog without the bridging six-membered ring in the side chain has been successfully prepared by submitting the all-*trans*-diazoketo to retinochrome, the isomerase present in squid eyes which transforms all-*trans*-retinal into 11-*cis*; isomerization occurred in 50% yield [21]. This photoaffinity label will now be incorporated into rhodopsin, and photoaffinity studies will be performed in liquid nitrogen to examine the cross-linking at the bathorhodopsin stage, *i.e.*, the first sequestable intermediate in the transduction process.

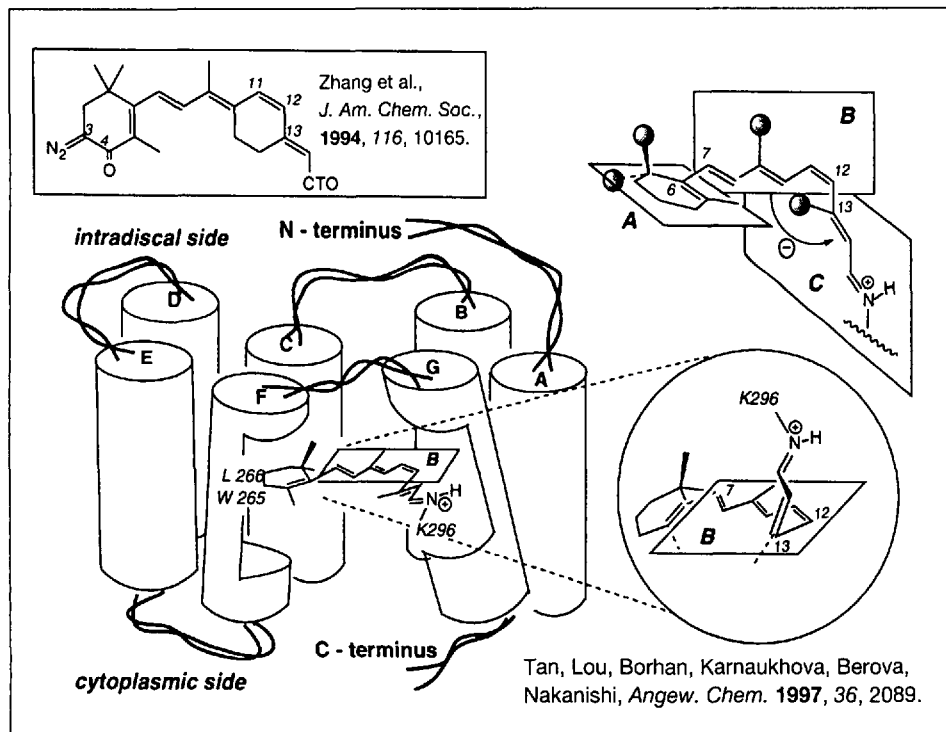


Fig. 8. Retinal site in rhodopsin under static dark state and its absolute twist around C(12)-C(13)

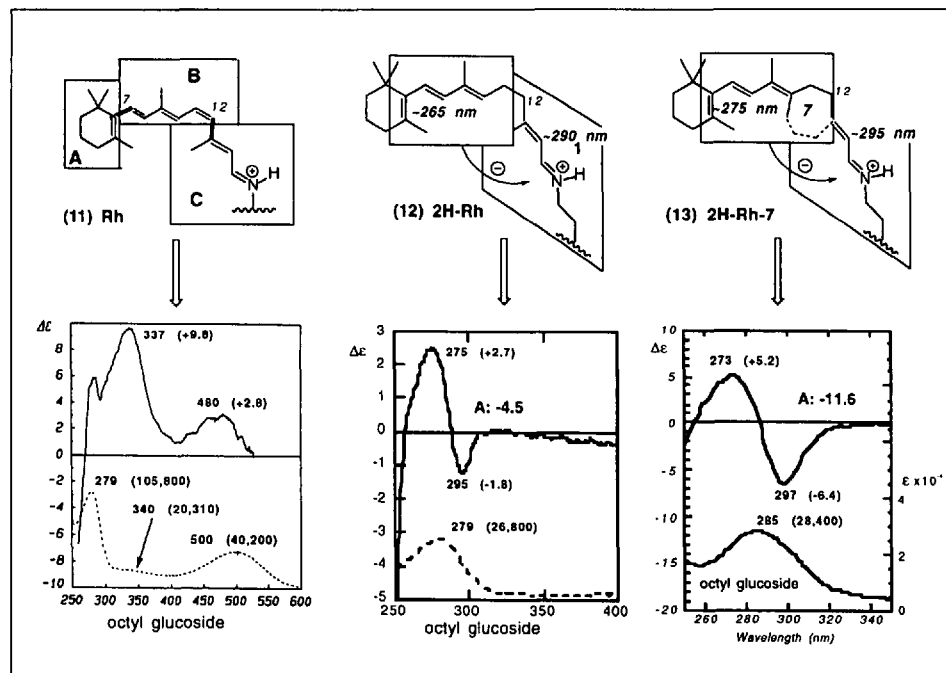


Fig. 9. UV/VIS and CD of rhodopsin (Rh, 11), dihydro-Rh (2H-Rh, 12), and dihydro-Rh-7 (2H-Rh-7, 13)

The absolute sense of twist around the C(12)-C(13) bond of the nonplanar 11-*cis*-chromophore [22] has a direct bearing on the subsequent transduction process. This was determined as follows [23]. The UV/Vis and CD spectra of bovine rhodopsin in octyl glucoside are shown in *Fig. 9*. Native rhodopsin, λ_{max} 500 nm, exhibits two positive CD Cotton effects at 480 nm

($\Delta\epsilon +2.8$, 'a-band') and 337 nm ($\Delta\epsilon +9.8$, 'b-band').

A twist of the polyene chain along the C(12)–C(13) single bond in retinal bound to rhodopsin does not produce an exciton-coupled CD because the polyene chain is conjugated throughout the molecule. However, saturation of the retinal 11-ene breaks the chromophore into two independent (dihomo-) conjugated systems, *i.e.*, the triene and the protonated Schiff's base (PSB) moieties. If the through-space interaction between these two chromophores in the pigment results in a couplet, then the sign of the split CD should reflect the absolute twist within the pigment binding site (Fig. 9). Provided 11,12-dihydroretinal adopts a conformation similar to 11-*cis*-retinal in rhodopsin, the exciton coupling between the triene and PSB should appear as either a positive or negative CD couplet depending on whether planes B and C constitute a positive or negative twist. The UV of 11,12-dihydroretinal (2H-Rh, 12) has one broad maximum centered around 279 nm in octyl glucoside; the accompanying CD shows negative and positive Cotton effects at 295 nm ($\Delta\epsilon -1.2$) and 275 nm ($\Delta\epsilon +2.5$), respectively, the *A* value being -4.5 . In contrast, the CD of native rhodopsin shows two positive Cotton effects (Fig. 9). Thus, the CD of 12 with negative/positive Cotton effects can be ascribed to the expected exciton coupling between the triene and PSB moieties. The results were further corroborated by the pigment incorporating the less flexible dihydroretinal analog with a seven-membered ring locking the 11-s-bond in cisoid form, 2H-ret-7 (13). It was shown earlier that the UV and CD spectra of the pigment obtained from the 11-*cis*-locked ret-7 closely resemble the UV and CD spectra of native rhodopsin, *i.e.*, the geometry of ret-7 within the binding site is very similar to that of native 11-*cis*-retinal [25]. Thus, the 13-*trans*-2H-ret-7 should be a more appropriate choice for a dihydro-11-*cis*-locked retinal analog. Indeed, the 2H-Rh-7 analog gave a similar negative couplet, but reflecting the less flexible structure of the chromophore the *A* value is now -11.6 . These results establish the absolute twist as depicted in Fig. 8. It is quite remarkable that the helicity between the triene and diene system within the protein binding site of the receptor is clearly reflected in the exciton-coupled CD spectra of the pigment.

We are extremely grateful to past and present group members who have produced all the results. The studies have been generously supported by various sources including NIH grants GM 34509, 36564, AI 10187.

Received: November 28, 1997

- [1] a) M. Maruyama, A. Terahara, Y. Itagaki, K. Nakanishi, *Tetrahedron Lett.* **1967**, 299; b) M. Maruyama, A. Terahara, Y. Itagaki, K. Nakanishi, *ibid.* **1967**, 303; c) M. Maruyama, A. Terahara, Y. Nakadaira, M.C. Woods, K. Nakanishi, *ibid.* **1967**, 309; d) M. Maruyama, A. Terahara, Y. Nakadaira, M.C. Woods, Y. Takagi, K. Nakanishi, *ibid.* **1967**, 315; e) M.C. Woods, I. Miura, Y. Nakadaira, A. Terahara, M. Maruyama, K. Nakanishi, *ibid.* **1967**, 321.
- [2] K. Nakanishi, *Pure Appl. Chem.* **1967**, *14*, 89.
- [3] K. Nakanishi, K. Habaguchi, Y. Nakadaira, M.C. Woods, M. Maruyama, R.T. Major, M. Alauddin, A.R. Patel, K. Weinges, W. Bähr, *J. Am. Chem. Soc.* **1971**, *93*, 3544.
- [4] T.A. van Beek, G.P. Lelyveld, *J. Nat. Prod.* **1997**, *60*, 735.
- [5] F.A.L. Anet, A.L.R. Bourn, *J. Am. Chem. Soc.* **1965**, *85*, 5250.
- [6] K. Nakanishi, K. Habaguchi, *J. Am. Chem. Soc.* **1971**, *93*, 3546.
- [7] M.K. Schwarz, Ph.D. Thesis, ETH-Zürich, Switzerland, 1994.
- [8] a) N. Harada, K. Nakanishi, 'Circular Dichroic Spectroscopy. Exciton Coupling in Organic Stereochemistry', University Science Books, Mill Valley, CA, 1983; b) K. Nakanishi, N. Berova, 'The Exciton Chirality Method', in 'Circular Dichroism: Principles and Applications', Eds. K. Nakanishi, N. Berova, R. Woody, VCH, New York, 1994, p. 361.
- [9] P. Zhou, N. Berova, W. Wiesler, K. Nakanishi, *Tetrahedron* **1993**, *49*, 9343.
- [10] I. Akritopoulou-Zanze, K. Nakanishi, H. Stepowska, B. Brzeszczyk, A. Zamojski, N. Berova, *Chirality* **1997**, *9*, 699.
- [11] a) D.H. Turner, I. Tinoco, Jr., M.F. Maester, *J. Am. Chem. Soc.* **1974**, *96*, 4340; b) I. Tinoco, Jr., D.H. Turner, *ibid.* **1976**, *98*, 6453.
- [12] J.-G. Dong, A. Wada, T. Takakuwa, K. Nakanishi, N. Berova, *J. Am. Chem. Soc.* **1997**, *119*, 12024.
- [13] a) Y.Y. Lin, M. Risk, S.M. Ray, D. van Engen, J.C. Clardy, J. Golik, J.C. James, K. Nakanishi, *J. Am. Chem. Soc.* **1981**, *103*, 6773; b) Y. Shimizu, H. Bando, H.-N. Chou, G. van Dyne, J.C. Clardy, *Chem. Commun.* **1986**, 1656; c) K.C. Nicolau, C.-K. Hwang, M.E. Duggan, D.A. Nugiel, T. Abe, K. Bal Reddy, S.A. DeFrees, D.R. Reddy, A.A. Awartani, S.R. Conley, F.P.J.T. Rutjes, E.A. Theodorakis, *J. Am. Chem. Soc.* **1995**, *117*, 10227.
- [14] a) S. Matile, K. Nakanishi, *Angew. Chem.* **1996**, *35*, 757; b) S. Matile, N. Berova, K. Nakanishi, *Chem.-Biol. Interact.* **1996**, *3*, 379.
- [15] a) A.T. Eldefrawi, M.E. Eldefrawi, K. Konno, N.A. Mansour, K. Nakanishi, E. Oltz, P.N.R. Usherwood, *Proc. Natl. Acad. Sci. U.S.A.* **1988**, *85*, 4910; b) T. Piek, R.H. Fokkens, H. Karst, C. Kruk, A. Lind, J. Van Marle, T. Nakajima, N.M.M. Nibbering, H. Shinozaki, W. Spanjer, Y.C. Tong, 'Neurotox '88: Molecular Basis of Drug & Pesticide Action', Ed. G.G. Lunt, Elsevier, Amsterdam, 1988, p. 61.
- [16] a) E.Y. Grishin, T.M. Volkova, A.S. Arseniev, O.S. Reshetova, V.V. Onoprienko, L.G. Magazanik, S.M. Antonov, I.M. Federova, *Bioorg. Khim.* **1986**, *12*, 1121; b) M.E. Adams, R.L. Carney, F.E. Enderlin, E.W. Fu, M.A. Jarema, J.P. Li, C.A. Miller, D.A. Schooley, M.J. Shapiro, V.J. Venema, *Biochem. Biophys. Res. Commun.* **1987**, *148*, 678; c) Y. Aramaki, T. Yasuhara, T. Higashijima, M. Yoshioka, A. Miwa, N. Kawai, T. Nakajima, *Proc. Japan. Acad., Ser. B* **1986**, *62*, 359; d) K.D. McCormick, J. Meinwald, *J. Chem. Ecol.* **1993**, *19*, 2411.
- [17] a) D. Huang, H. Jiang, K. Nakanishi, P.N.R. Usherwood, *Tetrahedron* **1997**, *53*, 12391, and ref. cit. therein; b) I.S. Blagbrough, E. Moya, S.P. Walford, *Tetrahedron Lett.* **1996**, *37*, 551.
- [18] K. Nakanishi, R. Crouch, *Israel J. Chem.* **1995**, *35*, 253, and ref. cit. therein.
- [19] a) H. Zhang, K. Lerro, T. Yamamoto, T. Lien, L. Sastry, M. Gawinowicz, K. Nakanishi, *J. Am. Chem. Soc.* **1994**, *116*, 10165; b) K. Nakanishi, H. Zhang, K. Lerro, S. Takekuma, T. Yamamoto, T. Lien, L. Sastry, D. Baek, C. Moquin-Pathey, M. Boehm, F. Derguini, M. Gawinowicz, *Biophys. Chem.* **1995**, *56*, 13.
- [20] T.A. Nakayama, H.G. Khorana, *J. Biol. Chem.* **1990**, *265*, 15762.
- [21] B. Borhan, R. Kunz, A. Y. Wang, K. Nakanishi, N. Bojkova, K. Yoshihara, *J. Am. Chem. Soc.* **1997**, *119*, 5758.
- [22] a) K. Nakanishi, *Am. Zool.* **1991**, *31*, 479; b) K. Nakanishi, *Pure Appl. Chem.* **1991**, *63*, 161; c) R.R. Rando, *Chem. Biol.* **1996**, *3*, 255.
- [23] Q. Tan, J. Lou, B. Borhan, E. Karnaukhova, N. Berova, K. Nakanishi, *Angew. Chem.* **1997**, *36*, 2089.
- [24] H. Akita, S.P. Tanis, M. Adams, V. Balogh-Nair, K. Nakanishi, *J. Am. Chem. Soc.* **1980**, *102*, 6370.